Skeletal Radiol (2014) 43:1205–1215
DOI 10.1007/s00256-014-1899-1

SCIENTIFIC ARTICLE

Thanatophoric dysplasia. Correlation among bone X-ray morphometry, histopathology, and gene analysis

Ugo E. Pazzaglia · Carla M. Donzelli · Claudia Izzi · Maurizia Baldi · Giuseppe Di Gaetano · MariaPia Bondioni

Received: 3 March 2014 / Revised: 8 April 2014 / Accepted: 21 April 2014 / Published online: 25 May 2014

Abstract
Objective Documentation through X-ray morphometry and histology of the steady phenotype expressed by FGFR3 gene mutation and interpolation of mechanical factors on spine and long bones dysmorphism.
Materials and methods Long bones and spine of eight thanatophoric dysplasia and three age-matched controls without skeletal dysplasia were studied after pregnancy termination between the 18th and the 22nd week with X-ray morphometry, histology, and molecular analysis. Statistical analysis with comparison between TD cases and controls and intraobserver/interobserver variation were applied to X-ray morphometric data.
Results Generalized shortening of long bones was observed in TD. A variable distribution of axial deformities was correlated with chondrocyte proliferation inhibition, defective seriate cell columns organization, and final formation of the primary metaphyseal trabeculae. The periosteal longitudinal growth was not equally inhibited, so that decoupling with the cartilage growth pattern produced the typical lateral spurs around the metaphyseal growth plates. In spine, platyspondyly was due to a reduced height of the vertebral body anterior ossification center, while its enlargement in the transversal plane was not restricted.

The peculiar radiographic and histopathological features of TD bones support the hypothesis of interpolation of mechanical factors with FGFR3 gene mutations.
Conclusions The correlated observations of X-ray morphometry, histopathology, and gene analysis prompted the following diagnostic workup for TD: (1) prenatal sonography suspicion of skeletal dysplasia; (2) post-mortem X-ray morphometry for provisional diagnosis; (3) confirmation by genetic tests (hot-spot exons 7, 10, 15, and 19 analysis with 80–90 % sensibility); (4) in negative cases if histopathology confirms TD diagnosis, research of rare mutations through sequential analysis of FGFR3 gene.

Keywords Thanatophoric dysplasia · X-ray morphometry · Endochondral ossification · Long bones and spine development

U. E. Pazzaglia (✉)
Orthopaedic Clinic, Department of Medical and Surgical Specialties, Radiological Sciences and Public Health, University of Brescia, Brescia, Italy
e-mail: ugo.pazzaglia@spedalicivili.brescia.it

C. M. Donzelli
Morbid Anatomy Department, Spedali Civili di Brescia, Brescia, Italy
e-mail: carladonzelli@yahoo.it

C. Izzi
Prenatal Diagnosis Unit, Department of Obstetrics and Gynaecology, University of Brescia, Spedali Civili, Brescia, Italy
e-mail: izziclaudia@yahoo.it

M. Baldi
Human Genetic Laboratory, Hospital Galliera, Genova, Italy
e-mail: m.baldi@galliera.it

G. Di Gaetano · M. Bondioni
Paediatric Radiology, Department of Medical and Surgical Specialties, Radiological Sciences and Public Health, University of Brescia, Brescia, Italy

G. Di Gaetano
e-mail: peppe11digaetano@hotmail.com

M. Bondioni
e-mail: mariapiabondioni@gmail.com

Introduction

Thanatophoric dysplasia (TD) is a short-limb dwarfism syndrome that is usually lethal in the perinatal period. TD is divided into type I, characterized by micromelia with bowed femurs and, uncommonly, the presence of cloverleaf skull

deformity (*Kleeblattschaedel*) of varying severity; and type II, characterized by micromelia with straight femurs and uniform presence of moderate-to-severe cloverleaf skull deformity. Other features common to type I and type II include: short ribs, narrow thorax, macrocephaly, distinctive facial features, brachydactyly, hypotonia, and redundant skin folds along the limbs. Most affected infants die of respiratory insufficiency shortly after birth. Rare long-term survivors have been reported. *FGFR3* is the only gene in which mutation is known to cause TD. The *FGFR3* mutation p.Lys650Glu has been identified in all individuals with TD type II [1–11]. Three variants of TD, defined as San Diego, Torrance, and Luton, have been described [12, 13]. The differential diagnosis was based on either radiographic or histological features. TD and San Diego variant present with similar radiologic aspects, such as micromelia, short ribs, platyspondyly, and the typical femurs deformity. Histologically, overgrowth of perichondral bone and ingrowth of mesenchymal tissue in the growth plate cartilage is present. However, metaphyseal cupping is more severe in San Diego type than in TD, while chondrocyte columns are better preserved in the former. FGFR3 mutation was documented in amniotic fluid of the San Diego variant [11].

Long bone shortening with or without bowing is a major sonographic sign used for prenatal diagnosis of several skeletal dysplasias including osteogenesis imperfecta, campomelic dysplasia, and thanatophoric dysplasia [1, 2, 8–10]. Fetal TD is suspected when shortened long bone or bowed femur along with narrow chest, short ribs, and macrocephaly is observed. Less severe X-ray bone abnormalities (particularly in femurs) can suggest a Torrance or a Luton variant. No FGFR3 mutation has been found in either [14].

Medial temporal lobe dysplasia is a frequently observed TD abnormality in prenatal sonography. Megalencephaly is generally present in 100 % of cases, with expansion of the temporal lobes along all the axes. It is associated with a prominent and deep transverse sulci in the temporal lobes [14–16]. However, a specific diagnosis is often difficult with only 40 % of cases being diagnosed correctly by 2D ultrasound as reported by Krakov in 2008 [17].

Therefore, gene analysis, standardized skeletal X-ray study, and bone histology are advised to confirm this genetic disease after pregnancy termination or delivery.

Radiographic morphometry allows a greater accuracy of measurements than clinical sonography and bone histology can be used to correlate the growth inhibition and the structural deformities caused by the endochondral ossification defect.

In the present study, a population of eight fetuses with X-rays and histopathological ascertained diagnosis of TD was examined. Skeletal X-rays were used to assess long bones and spine size parameters using as control the fetuses of age-matched pregnancy terminations with an ultrasonographic diagnosis of other disorders, which are not characterized by early skeletal dysmorphism.

The purpose of the paper was to document through X-ray morphometry and histology the steady phenotype expressed by the FGFR3 gene mutations, the possible interpolation of mechanical factors on spine and long bone dysmorphism, and to prompt a diagnostic workup in prenatal cases.

Materials and methods

Cases

Fetal ultrasound examination between the 15th and the 20th week of gestation revealed in eight cases shortened/or and bowed femur, narrow chest, and short ribs, which lead to a diagnosis of skeletal dysplasia resembling TD. The diagnosis was confirmed by genetic analysis of the *FGFR3* gene on fetal DNA in seven of the eight cases. One case (case #1 in Table 1) did not perform the analysis. Skeletal X-ray and histology supported the diagnosis in all cases including case #1. The control group included three fetuses with prenatal diagnosis of myelomeningocele, omphalocele, and hand agenesis, respectively. These voluntary pregnancy terminations were selected as controls for morphometric length assessment (Table 1).

In each of the cases, the parents chose to terminate the pregnancy, which was carried out between the 18th and the 22nd week of gestation. Consent for a complete autopsy was obtained from the parents and approval for further study was obtained from the Institutional Human Use Committee.

Molecular analysis: genomic DNA was isolated from amniocytes or chorionic villous. *FGFR3* exons 7, 10, 15, and 19 (hot spot regions for TD mutations) were amplified separately with 1 unit of EurobioTaq DNA polymerase (Eurobio) using a set of primers and PCR protocols defined in our laboratory. The PCR fragments were directly sequenced in both directions using the Big-Die-Terminator Cycle Sequencing kit (Applied Biosystems, Carlsbad, CA, USA). Sequencing reactions were purified with Multiscreen Filter Plates (Millipore Corporation, Bedford, MA, USA) and run and analyzed on a 3130xl Genetic Analyzer (Applied Biosystems).

X-rays

Fetus X-rays were performed before autopsy and were taken in lateral and antero-posterior views in a standardized position. The thorax and the limbs were secured to the X-ray digital panel surface with adhesive tape: upper limbs with 30° of shoulders abduction, extended elbows, and supinated hands. The lower limbs were positioned in neutral adduction unless there was severe bowing of the femurs, in which case the hips were abducted and extra-rotated in such a way that the bowed segment could lie as much as possible flat on the digital panel. The tube was kept at a distance of 1 m from the digital panel (Carestream DRX-1c System Detector, Ottawa, Canada), kV 50–55, 6.6 mA/

Table 1 Summary of thanatophoric dysplasia (TD) and control fetal cases

Case	Diagnosis	Pregnancy termination (weeks)	Weight (g)	[a]FGFR3 gene analysis (protein amino acid change)	Prenatal sonographic skeletal phenotype
1	TD type II	16	130	n/a	Shortening of the long bones, narrow chest, short and bowed ribs, bowed femurs and tibias
2	TD type I	17	178	[b]R248C	Shortening of the long bones narrow chest, short ribs, bowed femurs, *cloverleaf skull*
3	TD type I	20	340	P248C	Shortening of the long bones narrow chest, short ribs, bowed femurs, generalized edema
4	TD type I	20	345	S249C	Shortening of the long bones narrow chest, short ribs, bowed femurs
5	TD type II	21	380	K650E	Shortening of the long bones, narrow chest, short ribs, *cloverleaf skull*
6	TD type I	21	350	[b]Y373C	Shortening of the long bones, narrow chest, short ribs, bowed femurs, macrocephaly
7	TD type I	21	386	P248C	Shortening of the long bones, narrow chest, short ribs, bowed femurs, micrognathia
8	TD type I	22	400	[b]R248C	Shortening of the long bones, narrow chest, short ribs
9	Control	16	152	/	No skl malformation
10	Control	21	396	/	No skl malformation
11	Control	22	415	/	No skl malformation

[a] Mutation detection rate: 80 %

[b] Two most common mutations that account for almost 60–80 % of all TD type I

n/a not available

s. A reference scale was positioned on the panel margin to calibrate measurements on the X-ray image.

Skeletal X-ray morphometric assessment

X-ray images of the TD and control fetuses were retrospectively reviewed: those adequately demonstrating the fetal spine and the limbs long bones were selected for biometric assessment.

The length of the long bones ossified diaphyses was measured in the median longitudinal axis in straight bones (Fig. 1 a, b), while in the bent diaphyses, length was measured along the midline segmental arc (Fig. 1c). The assessed bone lengths on X-rays were the following: humeri, radii, ulnae, metacarpals, femurs, tibiae, and metatarsals.

The height of the ossified, anterior vertebral body was measured on the median line in both the antero-posterior and lateral projection X-rays of the spine (Fig. 2a–d). The height of the 9th, 10th, 11th, and 12th dorsal, and the 1st, 2nd, and 3rd lumbar was assessed. The ossified vertebral body height was calculated as the mean of the antero-posterior and lateral measurements. They were reported separately for the dorsal and lumbar tract.

Statistical analysis

The ossified vertebral body mean height and the long bones ossified diaphysis mean length (of both upper and lower limbs) were compared separately for individual right and left side bone between the TD population and the control group with Student's *t* test.

Repeated measurements were obtained independently by two radiologist investigators (MPB and GDG). Each single bone data set was measured twice at an interval of 1 month, resulting in two series of paired measurements. The differences of means analysis [18] was applied to these data sets. The difference of each pair of measurements (intraobserver and interobserver) was plotted against differences of long bone diaphysis length measurements (Fig. 3). Paired measurements of the ossified vertebral body height were plotted in the same mode. By analyzing the difference between the paired measurements, the only source of variability was the measurement error, which was likely to follow a normal distribution. The variation of the differences in all the interobserver data sets was wider than in the corresponding intraobserver sets, however with an acceptable degree of agreement (95 % confidence interval).

Bone histology

The selected bone specimens were fixed for 24 h in neutral, buffered formaldehyde solution (10 %) and then stored in a 4 % solution of the same fixative at 4 °C until processed. After decalcification in ethylene diamine tetraacetic acid (10 %) for

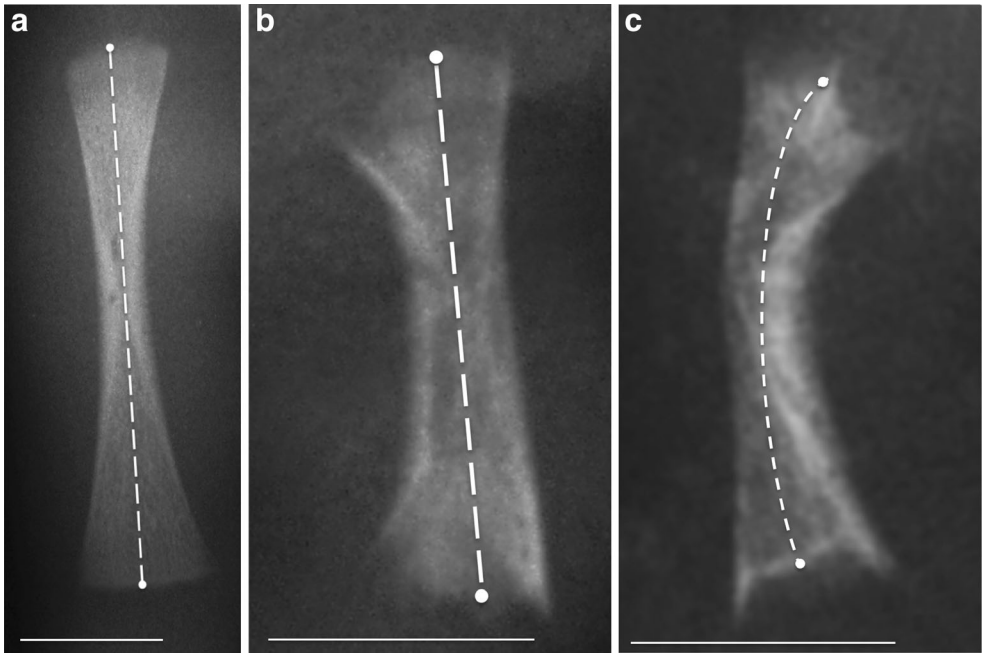

Fig. 1 **a** Control femur X-ray (gestational age 16 weeks). Method of measurement of the ossified diaphysis (*bar*=10 mm). **b** TD straight femur X-ray (gestational age 21 weeks). The ossified diaphysis is shorter than that of control and with an irregular structure of the cortex. The mid-shaft is enlarged by periosteal apposition around the diaphysis. The original shape of the diaphyseal ossification nucleus can be distinguished within the enlarged bone (*bar*=10 mm). **c** TD bent femur X-ray (gestational age 21 weeks). Method of measurement of the ossified bent diaphysis. Shortening and a thicker periosteal apposition are well evident on the concave margin as well as the spours on both the medial and lateral side of the growth plate cartilage (*arrows*) (*bar*=10 mm)

4 weeks, the specimens were dehydrated in an ascending scale of ethanol, embedded in paraffin, and 6–10-μm-thick sections were prepared with a microtome. Sections were carried out in the frontal plane of the epiphysis and the metaphysis to include the whole height of the growth plate cartilage; the diaphysis was sectioned longitudinally in five cases, while in one femur transversal sections were obtained at different levels from the growth plate to the mid-diaphysis. The spine was sectioned in the mid-sagittal plane of the vertebral bodies.

The sections were stained with hematoxylin and eosin (H&E), Weigert trichromic reaction for elastic fibers, and Alcian blue (pH 0.1 and 1.0) and observed with a light microscope Olympus BX 51 (Olympus Optical Ltd, Tokyo, Japan) equipped with an Image View telecamera (Soft Imaging System GmbH, Munster, Germany) in bright-field and in polarized light.

Results

Molecular analysis of genomic DNA carried out in seven of the eight cases revealed FGFR3 gene mutations (Table 1).

Skeletal X-ray morphometry and histopathology demonstrated that TD long bones were significantly shorter than those of the control group (compared between homologous bone), while differences between the right and left side of the same bone were not significant. Pathological bowing was never observed in any bone of the control group and in metacarpals and metatarsals of TD (Table 2). Bowing distribution was symmetrical in humeri, femurs, and tibiae (87.5 % or 85.7 % of the total); different right-left percentages were observed in the radii (87.5–100 %) and the ulnae (75–87.5 %). The distribution of bowed long bones in individual cases and for the single bones is reported in Table 3.

No epiphyseal ossification center has yet appeared in the TD group, as well as in the controls (gestational age from 18 to 22 weeks). The metaphyseal growth plate had a concave shape with more or less evident spurs on both the medial and lateral sides of the cartilage (Fig. 1b, c). The ossified diaphysis both in straight and bent bones did not have a normal cortex. The mid-shaft was enlarged by a periosteal apposition which appeared asymmetrical in bent bones. The original diaphyseal shape could still be recognized within, looking like two acute triangles united through the apex at mid-shaft level (Fig. 1b, c). The bowed bones had a thicker cortex on the concavity (Fig. 1c).

Histologically, there was little columnation of the growth plate chondrocytes, but the primary, metaphyseal trabeculae were also short. Whole sectors of the growth plate cartilage could be absent, being substituted by a layer of bone or otherwise calcified cartilage (Fig. 4a). Periosteal bone was formed around the edges of the growth plate cartilage, externally to the perichondral bone bark (Fig. 4b). This corresponded to the marginal bone spurs evidenced by X-

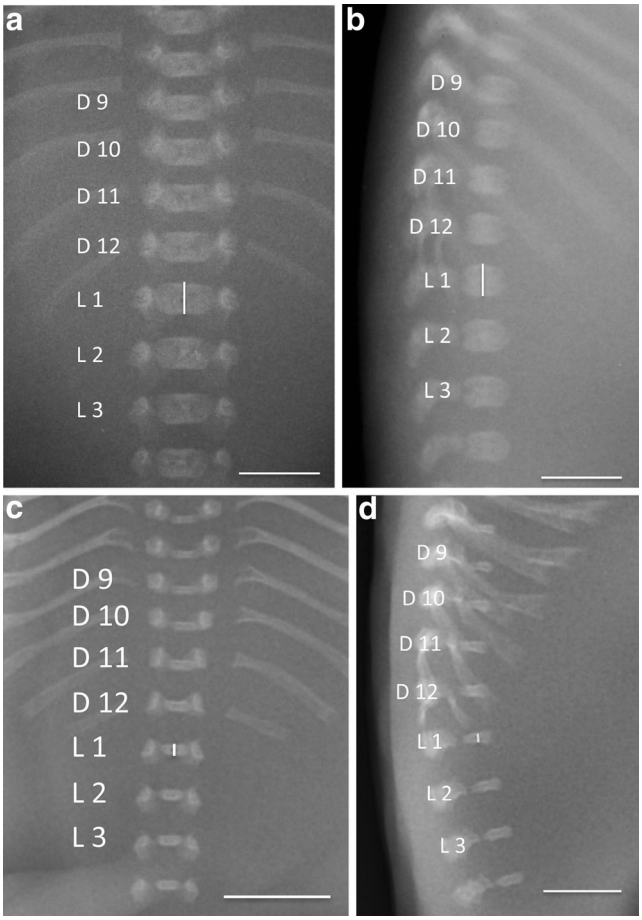

Fig. 2 **a**, **b** Control spine X-rays in antero-posterior and lateral projections (gestational age 17 weeks). The ossified anterior vertebral body is egg-shaped. The height of each body was measured on the median vertical line and reported as the mean of those of the two projections (*bar*=5 mm). **c**, **d** TD spine X-rays in antero-posterior and lateral projections (gestational age 21 weeks). The ossified anterior vertebral body is flattened on the vertical line, but there has been no such evident developmental inhibition in the transverse plane (*bar*=5 mm)

rays (Fig. 1b, c). The cortical bone in bent diaphyses was thicker on the concavity. Its structure suggested ongoing lamellar remodeling with vascular canals radially oriented on the concavity and nearly tangential to the periosteal surface of the convexity (Fig. 5).

In the spine, the ossified anterior vertebral body of TD had a rectangular shape in both the antero-posterior and lateral views. Those of the control group were oval-shaped.

The mean ossified vertebral body height was significantly lower in TD than in controls either at the level of the dorsal or lumbar tract (both $p<0.0001$). The difference between the dorsal and lumbar tract within either TD and the control group was not significant ($p=1.00$ and $p=0.46$, respectively) (Table 4).

The flat ossified vertebral body of TD corresponded to an asymmetric development of the ossification nucleus which had developed laterally in the frontal plane and antero-posteriorly in the lateral plane, but not along the longitudinal axis of the spine. Histology documented that the reduced height was due to a failure of chondrocyte column organization and primary trabeculae formation in this direction, while the expansion of the ossification nucleus was more regular in the transverse plane of the vertebra (Fig. 6a, b, c).

The chest was narrow with short ribs and posterior scalloping. There were no major alterations of the ribs' mineral density. The growth plate cartilage of the chondro-sternal junction showed a reduced height of the serial and hypertrophic chondrocyte layers in respect to controls. Also, the intercolumnar calcified septa appeared shorter or absent, and the differentiating osteoblasts had a limited space on the scaffold for formation of the primary metaphyseal trabeculae. Cortical lamellar structure of the ribs was well organized.

Small and short iliac bones with horizontal acetabular roofs. No histology was available.

It was not possible to perform an evaluation of the cranial bones' X-ray morphology because of the skull deformation induced by the surgical manipulation. Histology of calvaria membranous ossification in transverse sections was unremarkable.

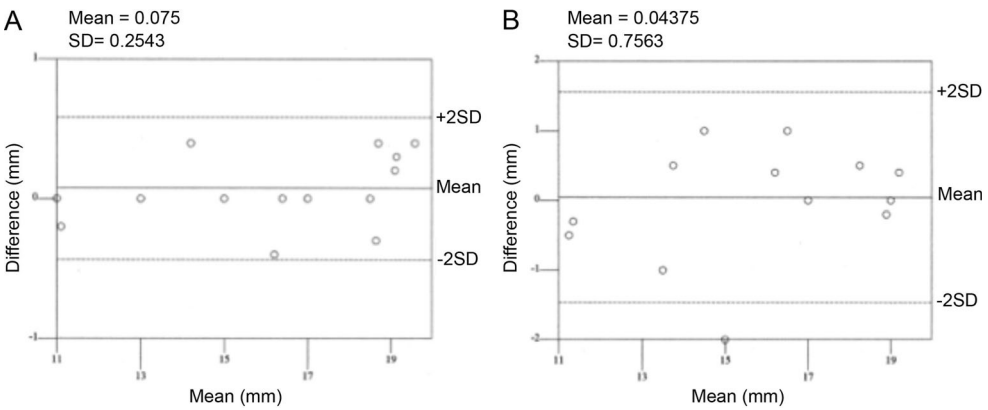

Fig. 3 Scatterplot shows mean of paired measurements (intraobserver) plotted against differences of TD humeral length measurements (**a**). *SD* standard deviation. Scatterplot shows mean of paired measurements (interobserver) plotted against differences of TD humeral length measurement (**b**). *SD* standard deviation

Table 2 Long bones biometric assessment: ossified diaphysis mean length comparison between thanatophoric dysplasia and the control group

	Thanatophoric dysplasia				Control group				
	n	Mean length (mm)[a]	Bowing[b] (%)	(*n*)	*n*	Mean length (mm)[a]	Bowing (%)[b]	(*n*)	*p* value
Humerus right	8	17.22±3.11	87.5 %	7	3	29.44±8.5	0 %	3	0.004
Humerus left	8	17.27±2.77	87.5 %	7	3	29.78±7.47	0 %	3	0.002
Radius right	8	13.28±2.62	87.5 %	7	3	25.33±7.69	0 %	3	0.003
Radius left	8	13.29±2.51	100 %	8	3	25.78±8.33	0 %	3	0.003
Ulna right	8	14.74±3.11	75 %	6	3	27.67±8.5	0 %	3	0.003
Ulna left	8	14.82±3.2	87.5 %	7	3	27.55±8.34	0 %	3	0.004
Metacarpals right	40	2.41±0.59	0 %	0	15	3.78±1.35	0 %	15	<0.0001
Metacarpals left	40	2.35±0.5	0 %	0	10	3.39±0.98	0 %	10	<0.0001
Femur right	8	17.6±4.41	87.5 %	7	3	30.11±8.17	0 %	3	0.008
Femur left	8	17.14±4.31	87.5 %	7	3	30±8	0 %	3	0.006
Tibia right	7	13.07±2.62	87.5 %	6	3	25.44±7,04	0 %	3	0.007
Tibia left	7	13.76±2.01	87.5 %	6	3	25±6.56	0 %	3	0.002
Metatarsals right	29	2.68±0.62	0 %	0	10	5±1	0 %	10	<0.0001
Metatarsals left	15	2.38±0.62	0 %	0	10	4.83±1.04	0 %	10	<0.0001

[a] Length given as mean ± SD separated for right and left side

[b] Bowing as % of total number of bones

Discussion

Descriptive TD radiographic aspects of the skeleton are well codified: they are based on five groups of malformations concerning the skull, the chest, the spine, the pelvis, and the long bones [19]. The definitive diagnosis of a prenatal skeletal dysplasia rests on biochemical and molecular techniques [3, 20]. However, the radiographic features of TD look remarkably homogeneous and recurrent; therefore, the diagnosis based on X-ray imaging alone has a very high reliability.

This lethal skeletal disorder has been associated with recurrent mutations in the fibroblast growth factor receptor 3 (FGFR3) gene. The genetic and biochemical studies have prompted a regulator's role for FGFR3 in embryos. It has been suggested that signaling through this factor both promotes and inhibits chondrocyte proliferation, depending on the time during development. The signal transducers and deactivators of the transcription (STAT 1) pathway is involved in the inhibition of chondrocyte proliferation, and the mitogen-activated protein kinase (MAPK) pathway in chondrocyte differentiation [21–23]. Chondrocytes have been reported in histopathological studies to be diminished in number and probable abnormal functionally [6, 24, 25]. In the present morphometric study, the most distinctive skeletal bone defect

Table 3 Single case distribution of axial deformities in thanatophoric dysplasia and controls

Case	Total long bones examined (*n*)	Bowed long bones (*n*)	Bowed long bones (%)	Bowed femurs (*n*)	Bowed humeri (*n*)	Bowed radii (*n*)	Bowed ulnae (*n*)	Bowed tibiae (*n*)	Bowed metacarpal (*n*)	Bowed metatarsal (*n*)
1	30	10/30	33.3	2/2	2/2	2/2	2/2	2/2	0/10	0/10
2	20	8/20	26.6	2/2	2/2	2/2	0/2	2/2	0/10	–
3	20	10/20	50	2/2	2/2	2/2	2/2	2/2	0/10	–
4	20	10/20	50	2/2	2/2	2/2	2/2	2/2	0/10	–
5	30	18/30	60	2/2	2/2	1/2	1/2	2/2	0/10	0/10
6	30	2/30	6.6	0/2	0/2	2/2	0/2	0/2	0/10	0/10
7	25	10/25	40	2/2	2/2	2/2	2/2	2/2	0/10	0/5
8	24	10/24	41.6	2/2	2/2	2/2	2/2	2/2	0/10	0/4
9	20	0/20	0	0/2	0/2	0/2	0/2	0/2	0/10	–
10	30	0/30	0	0/2	0/2	0/2	0/2	0/2	0/10	0/10
11	25	0/25	0	0/2	0/2	0/2	0/2	0/2	0/5	0/10

"–" indicates not assessable

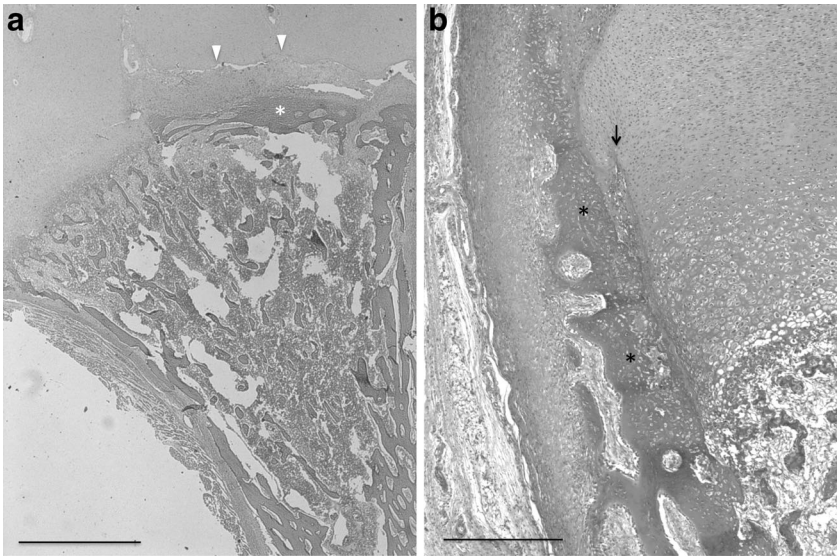

Fig. 4 **a** H&E stain of proximal tibial metaphysic (gestational age 21 weeks). The growth plate cartilage on the left half side shows an almost regular condrocyte columnation and primary metaphyseal trabeculae formation, but less dense than in control metaphyses. On the right half side, no endochondral ossification pattern is present. A transversal band of compact bone is interposed between the epiphysis and the metaphysic (*arrows*). In the epiphysis part of the cartilage is substituted by mesenchymal tissue (*arrowhead*) (*bar*=2 mm). **b** H&E stain, the bone deposed by the periosteum (*asterisk*) externally to growth plate cartilage and the perichondral bark (*arrow*) correspond to the X-ray image of the marginal metaphyseal spurs (see Fig. 1c) (*bar*=200 μm)

was a deficient longitudinal growth evident in either long bones or spine, significantly shorter than the corresponding bones of the control group.

The accurate positioning of the fetuses on the digital panel and the measurement methodology of the bent bones allowed reducing the projectional bias as it appears from variation of the length differences between the right and the left side. Intraobserver and interobserver variation were acceptable within the 95 % confidence interval.

The longitudinal length measurement of the ossified diaphysis is the most reliable X-ray morphometric method to evaluate a growth defect of the earlier diaphyseal ossification center and later of the metaphyseal growth plate cartilage. On the contrary, a reduced thickness of the growth plate cartilage often reported as an evidence of deficient chondrocyte differentiation and proliferation [6, 24, 26, 27] is not a direct index of the metaphyseal plate growth rate because the thickness of the chondrocyte columns is determined by the balance of the germinal layer proliferation rate and that of the vascular invasion/resorption from the metaphysis. Furthermore, quantitative assessment of the growth plate thickness in paraffin-embedded sections is subjected to the bias that the parallelism of microtome-cut sections with the chondrocyte columns cannot be accurately checked in paraffin-embedded sections.

The marginal overgrowth of the periosteal bone (external to the growth plate cartilage and the perichondral bone bark) is considered a typical X-ray and histologic sign of TD. However, its relevance in the evaluation of the longitudinal growth defect of long bones has not been so far completely appreciated. It can be observed not only in TD but also on other dysplasias characterized by micromelic development, like the Schneckenbecken dysplasia [28].

The long bones' regular, longitudinal growth is determined by the chondrocyte proliferation and their parallel lining in the seriate cell columns. Outside the perichondral bone bark, the periosteum also progresses in the longitudinal direction at the same rate of the condrocyte columns in normal developing subjects. Therefore the balance of the growth rate of these two structures is the factor conditioning the regular shape of the metaphysis [29]. The external spurs observed in the X-rays of

Table 4 Ossified anterior vertebral body mean height comparison between the same groups

	Thanatophoric dysplasia		Control group		
Ossified anterior vertebral body	*n*	Mean vertebral height (mm)	*n*	Mean vertebral height (mm)	*p* value
Dorsal	32	1.1±0.13	12	2.1±0.89	$p<0.0001$
Lumbar	24	1.1±0.23	9	2.4±0.92	$p<0.0001$
		$p=1.00$		$p=0.46$	

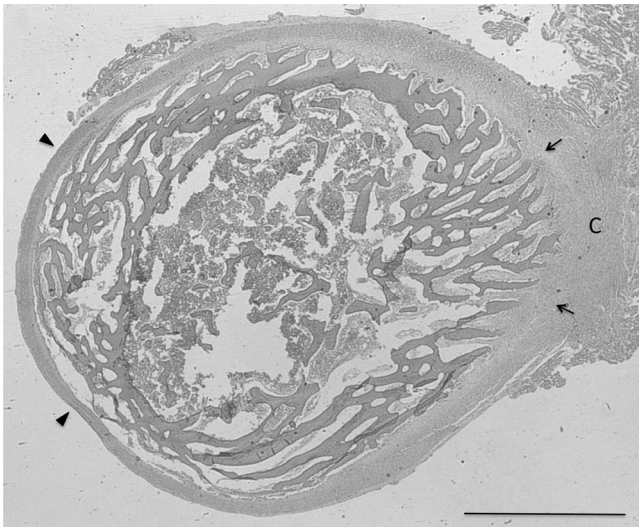

Fig. 5 H&E stain of TD diaphysis sectioned transversally, gestational age 21 weeks. Lamellar remodeling of the periosteal bone around oriented vascular canals. They were preferentially oriented along radial trajectories on the concave side of the diaphysis where the cortex was thicker (*arrows*), and became more tangential on the convex side (*arrowheads*) (*bar*=2 mm)

TD metaphyses or other micromelic dysplasias document a decoupling between the chondrocyte and the periosteal growth rate. On this basis, it is possible to link the phenotype "short long-bones" with the gene FGFR3 mutation, which induces a proliferation/organization inhibition of the chondrocytes [6, 21, 23].

Bowing of TD tubular bones is a less constant finding than shortening, and this led to the distinction between type 1 (bent long bones) and type 2, the less common straight bones form associated with cloverleaf skull [6, 30]. The analysis of the bent bones' distribution in each case of the TD population (Table 3) showed in two (fetuses 5 and 6) the presence of straight and bent bones in the same fetus, but this feature was not present in any metacarpal or metatarsal of the whole population. The variability of this character suggests that other environmental factors play a role on the determination of this dysmorphism, confirming the doubts of Kolbe et al. [3] that the distinction of two phenotype sub-types based on femoral bowing may be ambiguous.

A severe platyspondyly is typical of TD. Using as indicators the vertebral interspaces (a normalized indicator of the spine length calculated as the sum of the height of one ossified vertebra and the height of an adjacent un-ossified "disk space"), Rouse et al. [31] demonstrated a vertebral ratio for TD well below the range of normal spines, but also lower than those of achondroplasic fetuses. From the data of the present study, TD platyspondyly is peculiar because it associates the reduction of the height of the ossified anterior vertebral nucleus with a not-restricted peripheral enlargement in both the antero-posterior and the lateral views. Histology documented that the shape and the height of the whole cartilage model of the vertebral body was not different from the controls and only the ossified part was flattened.

The regular ossification centers of the controls were egg-shaped with the sequence of chondrocyte maturation producing a 3-D expansion of the ossifying nucleus [32, 33]. In TD, the column's orientation and expansion (when present) laid in perpendicular planes to the longitudinal axis of the spine. The

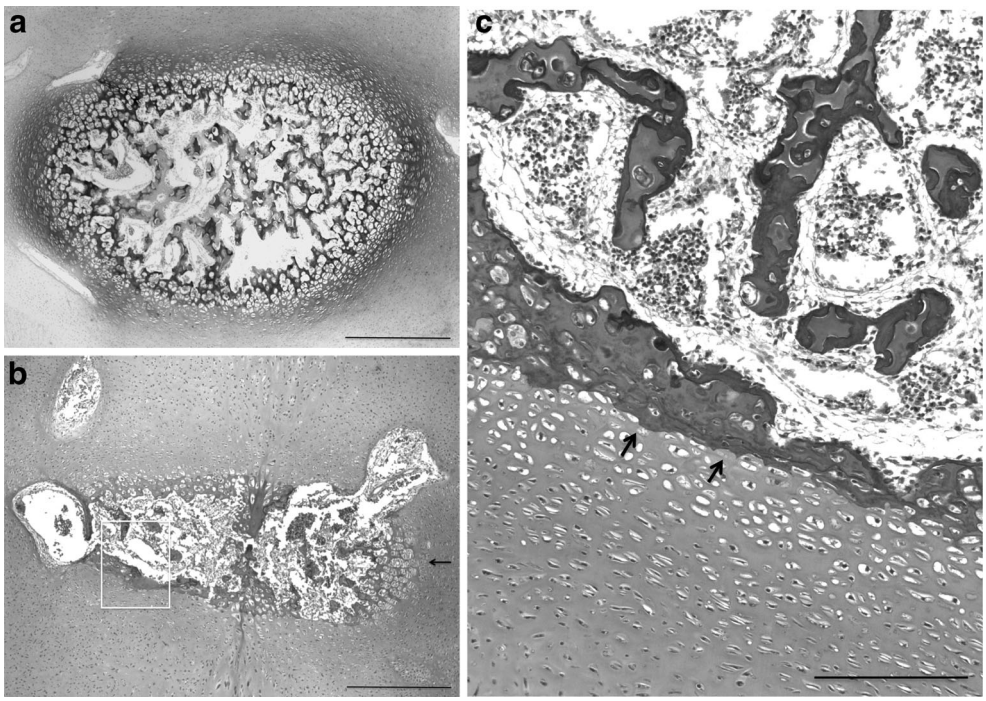

Fig. 6 **a** Hematoxylin and eosin (H&E) stain of control lumbar spine (gestational age 16 weeks). The ossified anterior vertebral body has an egg-like shape with chondrocyte columns and metaphyseal primary trabeculae 3-D oriented towards the center of the nucleus (*bar*=100 μm). **b** H&E stain, TD lumbar spine (gestational age 17 weeks). Chondrocyte columns asymmetry: they are well developed on the transverse plane perimeter (*arrow*) and are totally missing on the top and the bottom of the nucleus (*bar*=100 μm). **c** H&E stain, detail of the box in **b**. There is no columnation of the cartilage. Trabeculae with a calcified cartilage core have not been formed and they have been substituted by a transversal band of calcified cartilage (*arrow*) (*bar*=200 μm)

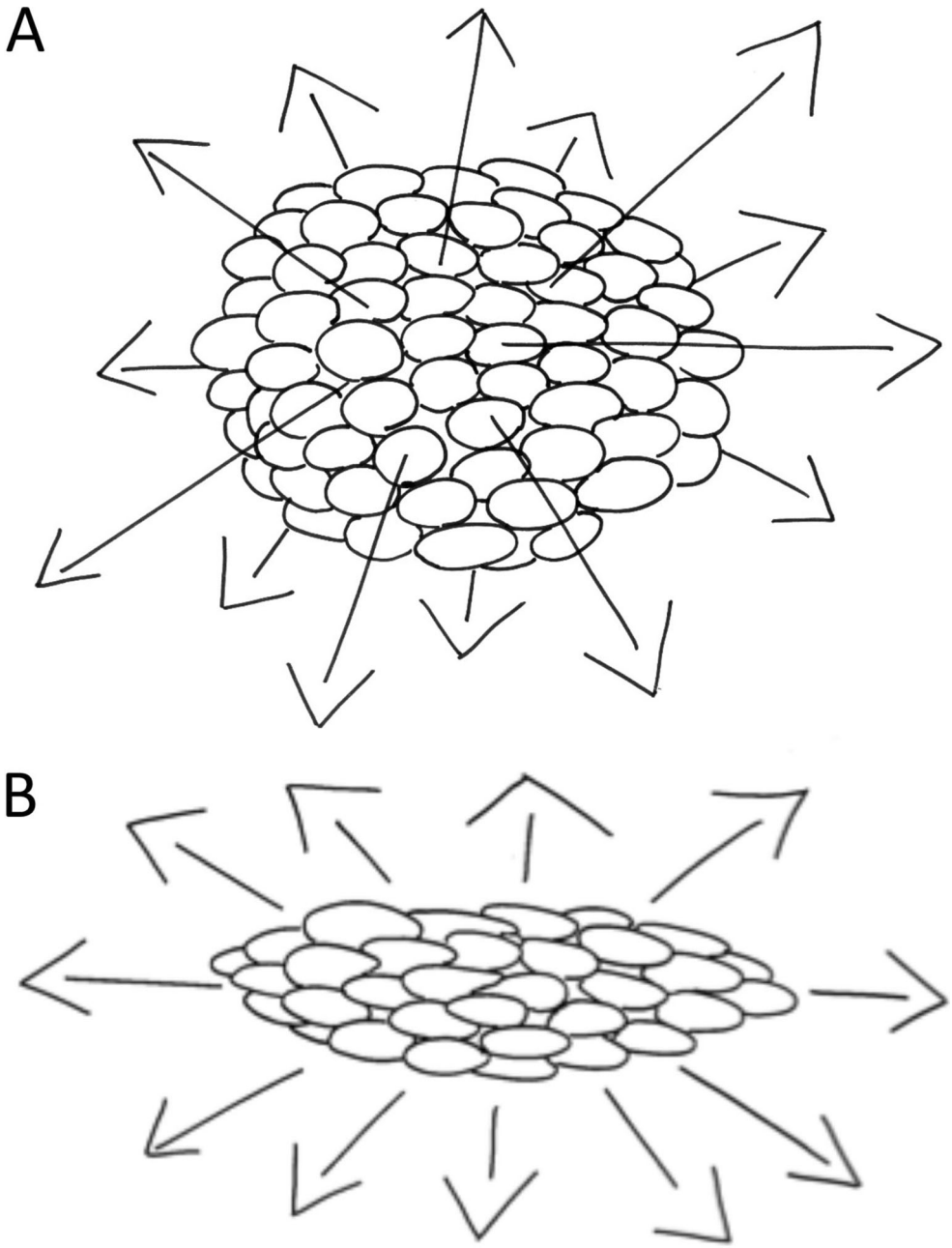

Fig. 7 Scheme suggesting the asymmetric effect of mechanical forces on the chondrocytes proliferation and 3-D organization of the vertebral anterior body ossification nucleus: **a** in the control nucleus chondrocytes proliferation and expansion is three-dimensionally oriented; **b** in thanatophoric dysplasia expansion is inhibited along the vertical direction

platyspondyly did not appear to be due to a collapse of the ossified nucleus, but rather to the spatial orientation of the columns, whose development was inhibited along the axial direction. Also, in the absence of fractures, a mechanical factor could be hypothesized (Fig. 7). Due to a higher compressive force oriented along the spine axis, a selective inhibition on a defective chondrogenesis can be hypothesized. The organization of the columns is based on the piling up of the cells of the cartilage germinative layer (proliferation) and the volume increment of the piled chondrocytes (hypertrophy). Therefore, the TD vertebral dysmorphism is also consistent with the cell-deficient proliferative and maturative processes conditioned by the gene FGFR3 mutation and with the weak mechanical strains acting along the spine longitudinal axis.

Early pathological studies of TD reported a normal membranous ossification and a generalized involvement of the endochondral ossification, with most of the chondrocytes forming columns with the aspect of "dark" cells and with no tendency of the "chief" cells to proliferate, to columnize, or to undergo hypertrophy [24]. Ornoy et al. [34] observed in TD growth plates areas with a less or more severe cartilage involvement, with tongues of mesenchymal tissue penetrating into the plate from the perichondrium or the periosteum. They also found small amounts of collagen III in some of the

TD infants, which were not present in the controls. They suggested, as a basic pathogenetic mechanism of the skeletal abnormalities, a focal replacement of the growth plate and periosteum by persisting abnormal mesenchymal-like tissue.

Horton et al. [35] also reported tufts of interstitial connective tissue into the growth plate cartilage which were interpreted as foci of a peculiar form of ossification (membranous) and supposed by these authors to be involved in the pathogenesis of the disorder.

Wilcox et al. [6], examining 57 cases of adequate histological sections of the long bones, observed a significant variability in the organization and length of the columns, the extent of the fibrous bands, and the metaphyseal bone abnormalities, with a wide spectrum extending from an almost normal growth plate pattern to no column formation. The fibrous bands could extend across the entire physis and the metaphyseal trabeculae be quite thick. These abnormalities were correlated with the abnormalities of the chondrocyte columns.

The histological observations of the present paper are consistent with the X-ray morphometric data and both support the hypothesis of the interpolation of mechanical factors with the gene-mediated defect of the osteochondral ossification [33]. Periosteal osteoblasts do not appear influenced by FGFR3 mutations, therefore the decoupling between chondrocyte and periosteal growth rate can explain the peculiar radiographic and histopathological features of TD bones.

The correlations of post-mortem X-ray morphometry, histopathology, and gene analysis observed in the present paper can support a diagnostic workup in four steps: (1) prenatal sonography suspicion of skeletal dysplasia; (2) post-mortem X-ray morphometry for provisional diagnosis of TD; (3) confirmation by genetic tests (hot-spot exons 7, 10, 15, and 19 analysis with 80–90 % sensibility; (4) in negative cases (from 10 to 20 %), if histopathology confirms TD diagnosis research of rare mutations through sequential analysis of FGFR3 gene.

Acknowledgments The work was supported by funding from the Department of Medical and Surgical Specialties, Radiological Sciences and Public Health of the University of Brescia. The authors acknowledge the contribution of the Scientific Committee of "Fondazione Mario Boni" in planning the study and drafting the paper, and counseling and suggestions from Prof. G. Beluffi, former Director of Pediatric Radiology of IRCCS Policlinico San Matteo, Pavia.

Conflict of interest The authors have no conflicts of interest to disclose.

References

1. Teele RL. A guide to the recognition of skeletal disorders in the fetus. Pediatr Radiol. 2006;36:473–84.
2. Alanay Y, Krakow D, Rimoin, Lachman RS. Angulated femurs and the skeletal dysplasias: experience of the International Skeletal Dysplasia Registry (1988–2006). Am J Med Genet. 2007;143A: 1159–68.
3. Kolbe N, Sobetzko D, Ersch J, Stallmach T, Eich G, et al. Diagnosis of skeletal dysplasia by multidisciplinary assessment: a report of two cases of thanatophoric dysplasia. Ultrasound Obstet Gynecol. 2002;19:92–8.
4. Miller E, Blaser S, Shannon P, Widjaja E. Brain and bone abnormalities of thanatophoric dwarfism. Am J Roentgenol. 2009;192:48–85.
5. Langer LO, Yang SS, Hall JG, Sommer A, Kottamasu SR, et al. Thanatophoric dysplasia and cloverleaf-skull. Am J Med Genet. 1987;3:167–9.
6. Wilcox WR, Tavormina PL, Krakow D, Kitoh H, Lachmann RS, et al. Molecular, radiologic, and histopathologic correlations in thanatophoric dysplasia. Am J Med Genet. 1998;78:274–81.
7. Hall BD, Spranger J. Congenital bowing of the long bones. Eur J Pediatr. 1980;133:131–8.
8. Goncalves L, Jeanty P. Fetal biometry of skeletal dysplasias: a multicentric study. J Ultrasound Med. 1994;13:977–85.
9. Schild RL, Hunt GH, Moore J, Davies H, Horwell DH. Antenatal sonographic of thanatophoric dysplasia: a report of three cases and a review of the literature with special emphasis on the differential diagnosis. Ultrasound Obstet Gynecol. 1996;8:62–3.
10. Donnelly DE, McConnell V, Paterson A, Morrison PJ. The prevalence of thanatophoric dysplasia and lethal osteogenesis imperfecta type 2 in Northern Ireland. A complete population study. Ulster Med J. 2010;79:114–8.
11. Kitoh H, Lachman RS, Brodie G, Mekikian PB, Rimoin DL, Wilcox WR. Extra pelvic ossification centers in thanatophoric dysplasia and platyspondylic lethal skeletal dysplasia-San Diego type. Pediatr Radiol. 1998;28:759–63.
12. Horton WA, Rimoin DL, Hollister DW, Lachmann RS. Further heterogeneity within lethal neonatal short-limbed dwarfism, the platyspondylic types. J Pediatr. 1979;94:736–42.
13. Winter RM, Thompson EM. Lethal neonatal, short-limbed platyspondylic skeletal dysplasia. A further variant? Hum Genet. 1982;61:269–72.
14. Neumann L, Kunze J, Uhl M, Stover B, Zabel B, Spranger J. Survival to adulthood and dominant inheritance of platyspondylic skeletal dysplasia, Torrance-Luton type. Pediatr Radiol. 2003;33:786–90.
15. Vogt C, Blaas HG. Thanatophoric dysplasia: autopsy findings over a 25-year period. Pediatr Dev Pathol. 2013;16:160–7.
16. Blaas HGK, Vogt C, Eik-Nes SH. Abnormal gyration of the temporal lobe and myelencephaly are typical features of thanatophoric dysplasia and can be visualized prenatally by ultrasound. Ultrasound Obstet Gynecol. 2012;40:230–4.
17. Krakow D, Alanay Y, Rimoin LP, Lin V, Wilcox WR, Lachman RS, et al. Evaluation of prenatal-onset osteochondrodysplasias by ultrasonography: a retrospective and prospective analysis. Am J Med Genet A. 2008;146A:1917–24.
18. Bland JM, Altman DG. Statistical methods for assessing agreement between two methods of clinical measurement. Int J Nurs Stud. 2010;47:931–6.
19. Hall CM, Offiah AC, Forzano F, Lituania M, Fink M. Fetal and perinatal dysplasia. An atlas of multimodality imaging. London: Radcliffe Medical Press LTD; 2012.
20. Chitty LS, Khalil A, Barret AN, Pajkrt E, Griffin DR, Cole JJ. Safe, accurate, prenatal diagnosis of thanatophoric dysplasia using ultrasound and free fetal DNA. Prenat Diagn. 2013;14:1–8.
21. Iwata T, Chen L, Li C, Ovchinnikov DA, Behringer RR, et al. A neonatal lethal mutation in FGFR3 uncouples proliferation and differentiation of growth plate chondrocytes in embryos. Hum Mol Genet. 2000;9:1603–13.
22. Lievens PM, Liboi E. The thanatophoric dysplasia type II mutation hampers complete maturation of fibroblast growth factor receptor 3 (FGFR3), which activates signal transducer and activator of

transcription 1 (STAT1) from the endoplasmic reticulum. J Biol Chem. 2003;278:17334–9.
23. Martinez-Frias ML, de Frutos CA, Bermejo E, Nieto MA. ECEM Working Group Review of the recently defined molecular mechanisms underlying thanatophoric dysplasia and their potential therapeutic implications for achondroplasia. Am J Med Genet. 2010;152A:245–55.
24. Hwang WS, Tock EPC, Tan KL, Tan LKA. The pathology of cartilage in chondrodysplasias. J Pathol. 1979;127:11–8.
25. Briner J, Giedion A, Spycher MA. Variation of quantitative and qualitative changes of endochondral ossification in heterozygous achondroplasia. Pathol Res Pract. 1991;187:271–8.
26. Weber M, Johansson R, Carstens C, Pauschert R, Niethard FU. Thanatophoric dysplasia type II: new entity? J Pediatr Orthop B. 1998;7:10–22.
27. Mancilla EE, De Luca F, Uveda JA, Czerwiec FS, Baron J. Effects of fibroblast growth factor-2 on longitudinal bone growth. Endocrinology. 1998;139:2900–4.
28. Nikkels PG, Stigter RH, Knol IK, van der Harten HJ. Schckenbecken dysplasia, radiology, and histology. Pediatr Radiol. 2001;31:27–30.
29. Pazzaglia UE, Beluffi G, Benetti A, Bondioni MP, Zarattini G. A review of the actual knowledge of the processes governing growth and development of long bones. Fetal Pediatr Pathol. 2011;30:199–208.
30. Lee SH, Cho JJ, Song MJ, Min JY, Han BH, et al. Fetal musculoskeletal malformations with a poor outcome: ultrasonographic, pathologic, and radiographic findings. Korean J Radiol. 2002;3:113–24.
31. Rouse GA, Filly RA, Toomey F, Grube L. Short-limb skeletal dysplasias: evaluation of the fetal spine with sonography and radiography. Radiology. 1990;174:177–80.
32. Pazzaglia UE, Salisbury JR, Byers PD. Development and involution of the notochord in the human spine. J R Soc Med. 1989;28:413–5.
33. Pazzaglia UE, Bonaspetti G, Rodella LG, Ranchetti F, Azzola F. Design, morphometry and development of the secondary osteonal system in the femoral shaft of the rabbit. J Anat. 2007;211:303–12.
34. Ornoy A, Adomian GE, Eteson DJ, Burgeson RE, Rimoin DL. The role of mesenchymal-like tissue in the pathogenesis of thanatophoric dysplasia. Am J Med Genet. 1985;21:613–30.
35. Horton WA, Hood OJ, Machado MA, Ahmed DS, Griffey ES. Abnormal ossification in thanatophoric dysplasia. Bone. 1988;9:53–61.